Dynamic storage function by chaos control in a hybrid bistable system

Ying Zhang,[2] Jian-Bin Li,[2] Zhi-Ren Zheng,[2] Yun Jiang,[2] and Jin-Yue Gao[1,2,*]
[1]*CCAST (World Laboratory), P.O. Box 8730, Beijing 100080, China*
[2]*Physics Department, Jilin University, Changchun, Jilin 130023, China*
(Received 4 April 1997)

Two methods of chaos control in a dynamic storage device which has been realized in an electro-optical bistable system pumped by a He-Ne laser are proposed. Experimental result agrees with the theoretical simulations and the Lyapunov exponent analysis. Up to 55 bits binary data storage have been successfully demonstrated. [S1063-651X(98)14502-6]

PACS number(s): 05.45.+b, 42.65.Sf, 42.79.Vb, 42.65.Pc

I. INTRODUCTION

Theoretical and experimental studies on delayed feedback systems have shown the existence of a variety of multistable bifurcated harmonic oscillation modes leading to chaos [1–8]. The potential applicability for large capacity optical signal storage using this phenomenon has been suggested [3]. Two methods, seed signal injection and chaotic search, for coding of the bifurcated harmonic oscillations have been proposed by Davis and Ikeda [4–6], and have been studied in both computer simulation and experiment by Aida and Davis [7–9]. This research gave a concrete image to the usefulness of this nonlinear phenomenon. Using the seed signal injection method, Gao *et al.* have stored binary codes into an electro-optical bistable system, and storage up to 51 bits has been realized [10].

The seed signal injection method is the direct, deterministic selection of a mode by injection of a signal close to the mode. The chaotic search method is an approach that adjusts the adaptive parameter of bifurcation to and from the chaos region to a selected mode.

The seed signal injection is limited by its direct selection and seed injection in advance when a desirable code needs to be stored into the system, and the chaotic search method forces system parameters into jumping from one state to another, which could bring additional influence into the system.

In this paper we present two methods of chaos control which apply continuous self-controlling feedback into dynamic information storage. Theoretical analyses and computer simulation have shown the validity of these methods. Experimental demonstrations will be presented which agree with the theoretical analyses.

II. TWO METHODS OF CHAOS CONTROL FOR DYNAMIC STORAGE

Figure 1 shows a schematic diagram of an electro-optical bistable system. The system considered is composed of a light source, modulator, and a feedback loop with large delay time. Its dynamic behavior can be described by the following dimensionless equation [10]:

$$\frac{dV(t)}{dt} = -V(t) + \frac{1}{2} I_1\{1 - k\ \cos[V(t-T)+\theta]\} = f(t), \tag{1}$$

where I_1 and $V(t)$ represent the input and output intensity levels, and $V(t)$ is proportional to the feedback voltage; T is the effective delay time in feedback loop, θ measures, in units of the half-wave voltage, the fixed bias applied to the electro-optical element, and k is the modulation depth of the device. Both T and the time variable t are scaled to the natural response time of the hybrid bistable system.

The system could get into chaos via a complicated way with increasing the bifurcation parameter (for example, input intensity) as described in Ref. [3], and we get the bifurcation diagram of output oscillation levels without chaos control by solving Eq. (1) numerically as shown in Fig. 2. In the bifurcation region of $m=2$ in Fig. 2, multistable periodic oscillation solutions coexist, and each has a certain number of independent competitive patterns that we called isomers [8]. We can completely identify a wave form of the $(n,m=2)$ class by assigning 1-bit binary labels 0 or 1 to the peak levels in a $2T$ interval, so that different solutions have different peak modulation. For example, there are ten types of isomers for the solutions of the $(n=7,m=2)$ class [8,10], and their oscillation wave forms are regular. In the inverse bifurcation region of $m^*=2^*$ in Fig. 2, multiple unstable periodic oscillation solutions coexist too, and each has a certain number of independent chaotic competitive patterns. For example, ten types of isomers also coexist for the solutions of the $(n=7,m^*=2^*)$ class, and their oscillation wave forms are chaotic. Chaotic itinerancy exists in the inverse bifurcation

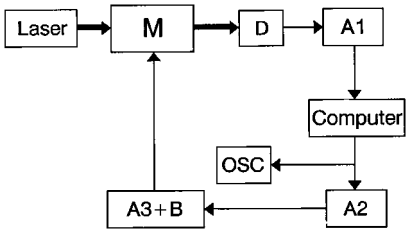

FIG. 1. Schematic diagram of an electro-optical bistable system. M:$LiNbO_3$ crystal modulator; D: detector; $A1$,$A2$,$A3$: amplifier; B: bias voltage; Osc: oscilloscope; Laser: He-Ne laser source; Computer: delay and chaos control system.

*Electronic address: jygao@mail.jlu.edu.cn

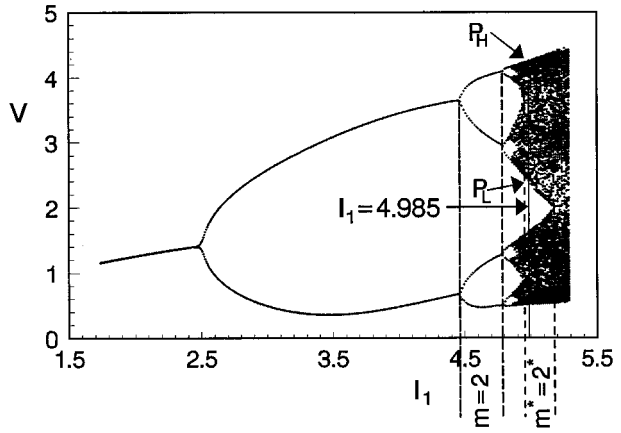

FIG. 2. Bifurcation diagram of output oscillation level without chaos control. The parameters used are $k=0.8$, $\theta=\pi$, $T=100$, $X=0.0$. $I_1=4.985$ is the operating point of dynamic memory. P_H and P_L are the maximum and the minimum values of higher and lower peak at $I_1=4.985$.

region of $m^*=2^*$, for example, where intermittent chaotic mode transitions occur persistently among all the ten isomers of the $(n=7,m^*=2^*)$ class, and these isomers will appear one after another in chaotic itinerancy [9]. From above, we know that it is possible to make use of coexisting isomers to store complex information as temporal patterns.

In this work, the system operates in the developing chaotic region where it has the solutions of the $(n,m^*=2^*)$ class. We adopted two methods of chaos control by continuous self-controlling feedback in dynamic storage. One is delayed feedback control, $F(t)=X[V(t-T)-V(t)]$, that appears similar to the method proposed by Pyragas and Tamasevicius [11,12]. In the Pyragas method, the delay time in the control signal is usually coincident with the period of the target oscillation in the original system, and at the same time it was pointed out that the output oscillation can be chaotic or periodic when the delay time in the control signal differs considerably from the period of the unstable periodic orbits in the Rösser system. In this paper, the delay time used in the control signal is T, which is just the delay time in feedback loop of the original system. The other is output feedback control, $F(t)=X[-V(t)]$, that was proposed by Davis [5]. The block diagrams of the two methods are shown in Fig. 3.

III. ANALYSIS AND SIMULATION OF THE TWO METHODS

The dynamic equation of the system under chaos control can be written as

$$\frac{dV(t)}{dt}=f(t)+F(t)=\begin{cases}X[V(t-T)-V(t)],\\ X[-V(t)].\end{cases} \tag{2}$$

We found that slightly modifying weight X can change chaos into regularity in the inverse bifurcation region of $m^*=2^*$. In order to justify the validity of the two methods in the system under consideration, we carried out an analysis of the first Lyapunov exponent.

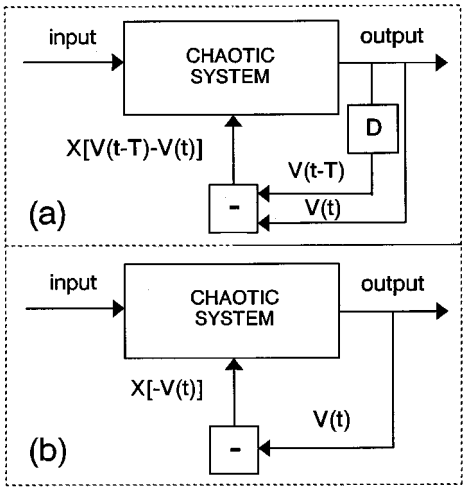

FIG. 3. Block diagram of (a) delayed feedback control, $F(t)=X[V(t-T)-V(t)]$, and (b) output feedback control, $F(t)=X[-V(t)]$, D is delay system, X is control weight.

Let $0<\tau\leqslant T$, $t=(N-1)T+\tau$; then $V_N(\tau)=V(t)$, and $dV(t)/dt\approx 0$ with large T, and Eq. (2) can be approximated to the following equation:

$$V_{N+1}(\tau)=\frac{WV_N(\tau)+\frac{1}{2}I_1\{1-k\cos[V_N(\tau)+\theta]\}}{1+X}, \tag{3}$$

where $W=X$ when $F(t)=X[V(t-T)-V(t)]$, or $W=0$ when $F(t)=X[-V(t)]$.

Along with the Lyapunov exponent analysis in Ref. [3], the first Lyapunov exponent is determined by

$$\lambda_1=\max_{\{0<\tau\leqslant T\}}\left\{\lim_{N\to\infty}\frac{1}{N}\sum_{i=1}^{N}\ln\left|\frac{W+\frac{1}{2}I_1k\sin[V_N(\tau)+\theta]}{1+X}\right|\right\}. \tag{4}$$

Figure 4 shows the first Lyapunov exponents of the output oscillation for both cases. It is clear that the first Lyapunov

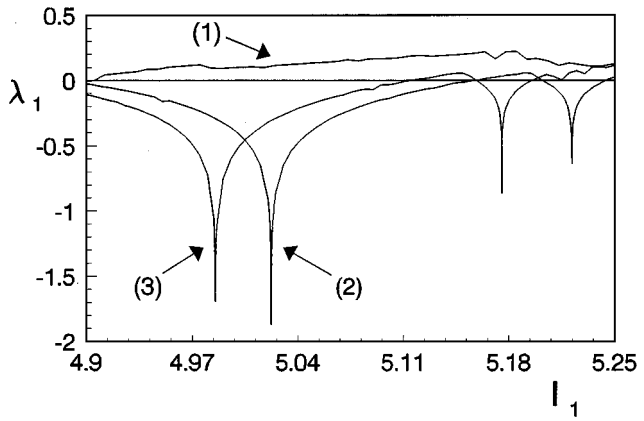

FIG. 4. Lyapunov exponent versus I_1 in the inverse bifurcation region of $m^*=2^*$. The parameters used are $k=0.8$, $\theta=\pi$, $T=100$. (1) Without chaos control, $X=0.0$, (2) with delayed feedback control, $F(t)=X[V(t-T)-V(t)]$, $X=0.066$, (3) with output feedback control, $F(t)=X[-V(t)]$, $X=0.066$.

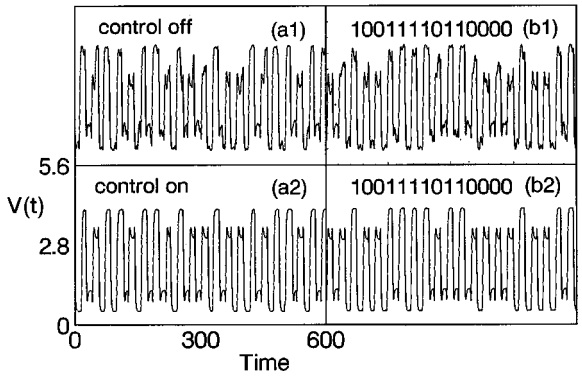

FIG. 5. The computer simulation of dynamic memory by chaos control in the inverse bifurcation region of $m^*=2^*$. The parameters used are $k=0.8$, $\theta=\pi$, $T=100$, $I_1=4.985$, $X=0.05$, $n=7$. (a) With delayed feedback control, $F(t)=X[V(t-T)-V(t)]$, (b) with output feedback control, $F(t)=X[-V(t)]$.

exponents could become negative after chaos control in a wide parameter range while they are positive before the control. This indicates that the chaos oscillation in the inverse bifurcation region of $m^*=2^*$ is greatly suppressed by the continuous self-controlling feedback. The comparison between curves (2) and (3) in Fig. 4 shows that the two methods are equally effective for dynamic storage, and the output feedback control is simpler than the delayed feedback method, because it does not require any delayed signal. The only difference between them is that the operating region is slightly shifted.

The theoretical simulation demonstrates the effectiveness of the two methods for dynamic storage. Figure 5(a) shows the oscillation wave forms of a code of the seventh harmonic modes before and after the delayed feedback control, and Fig. 5(b) shows the oscillation wave forms of another code of the seventh harmonic modes before and after the output feedback control. It is obvious that the two methods are both very effective.

Figure 6 is a bifurcation diagram of output oscillations when the delayed feedback control was used. It shows that the whole bifurcation diagram was shifted to the right-hand side comparing with the diagram in Fig. 2 where control was not used. The operating point $I_1=4.985$, as an example, is in the bifurcation region of $m=2$ in Fig. 6, while it was in the inverse bifurcation region of $m^*=2^*$ in Fig. 2. In the calculation, a very small value of control weight $X=0.0594$ was used. A similar calculation was done for the output feedback control, and the results are the same. The above calculations also show the reason why the two methods used here could change the chaotic oscillation codes into regular oscillation.

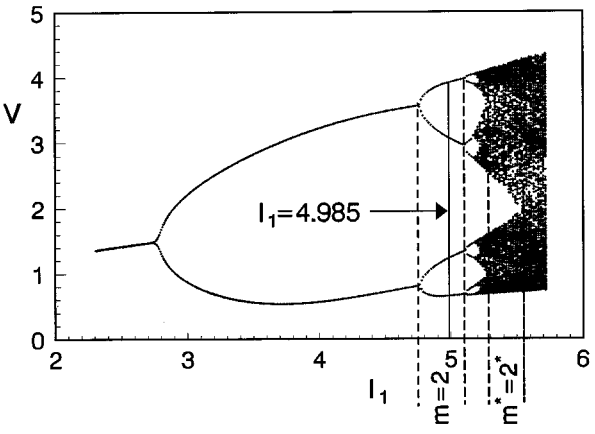

FIG. 6. Bifurcation diagram of output oscillation level with delayed feedback control, $F(t)=X[V(t-T)-V(t)]$, in the inverse bifurcation region of $m^*=2^*$. The parameters used are $k=0.8$, $\theta=\pi$, $T=100$, $X=0.0594$. $I_1=4.985$ is the operating point of dynamic memory.

IV. EXPERIMENT, RESULTS, AND DISCUSSION

We carried out our experiments in an electro-optical bistable system shown schematically in Fig. 1. A 3-mV He-Ne laser is used as the input, which is detected by a photomultiplier D after going through a modulator M made from $LiNbO_3$. The electric signal from D is amplified by three amplifiers and delayed by a computer. The output feedback signal together with a fixed bias and the control signal produced by the computer are applied to the modulator M. The computer is also used for data input, and the output data record. The output oscillation of the system is monitored by an oscilloscope.

With the above setup, we measured the open-loop relaxation time of the system by applying a square-wave signal to the system and recording the rise and delay time of the distorted wave form at the modulator M. The actual delay time was set to be zero in this measurement, and the natural response time measured is $\tau_r=0.11\pm0.01$ ms. We also timed the sampling of the computer, and it is 0.038 ± 0.001 ms.

The procedure of dynamic storage by chaos control is as follows. As an example, we set the actual delay time T_r to 5.32 ms (the effective delay time is $T=T_r/\tau_r=48.36$), and store oscillation code data of the $(n=7,m=2)$ class by the computer in a T interval. The peak and valley values in the code are the same as the corresponding values in the $(n=1,m=2)$ oscillation wave forms of the system, which can be read from the computer before the signal is produced. Then, we close the loop of the system and tune the input intensity and bias voltage until the system operates in the inverse bifurcation region of $m^*=2^*$. When the system is in operation, it visits all the ten isomers of the seventh harmonic mode randomly. During this time, the maximum and the minimum value, P_H and P_L as shown in Fig. 2, of higher and lower peaks of output oscillation have been searched and stored by the computer, and we set $D=(P_H+P_L)/2$. Then the average value P_i for each peak (about 20 data) is calculated and compared with D one by one. If $P_i>D$, it will be designated as 1, otherwise it will be designated as 0. We compared the code consisting of P_i series in a period of $4T$ with the target code, for example, (10011110110000) as seen in Fig. 5(b2). If the code is not the same as the target code, we move to the next code which is beginning from the second peak in the previous code until the code which is the same as the target code is found as seen in Fig. 5(b1). We switch on the chaos control and the code is stored into the system. The oscillation code could be erased by switching the chaos control off. The next selected code could be stored in the same way.

We demonstrated the two methods described in Sec. III

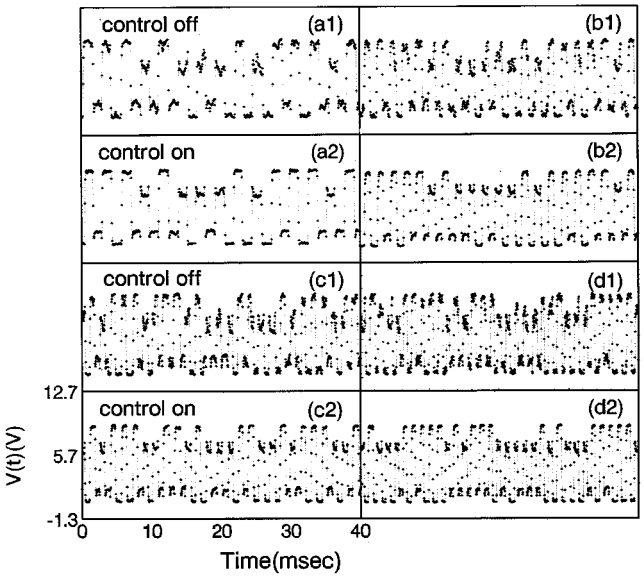

FIG. 7. Four examples of experimental results of dynamic memory by chaos control in the inverse bifurcation region of $m^*=2^*$. (a) and (b) with the delayed feedback control of $F(t)=X[V(t-T)-V(t)]$, (c) and (d) with the output feedback control of $F(t)=X[-V(t)]$. The parameters used are (a) $T_r=3.99$ ms, $n=5$, (b) $T_r=5.32$ ms, $n=7$, (c) $T_r=6.84$ ms, $n=9$, (d) $T_r=8.36$ ms, $n=11$.

experimentally in the inverse bifurcation region of $m^*=2^*$ and the results are shown in Fig. 7. Figures 7(a) and 7(b) show the coded oscillation wave forms of the $(n=5,m^*=2^*)$ and $(n=7,m^*=2^*)$ class using delayed feedback control, and Figs. 7(c) and 7(d) show the coded oscillation wave forms of the $(n=9,m^*=2^*)$, $(n=11,m^*=2^*)$ class using

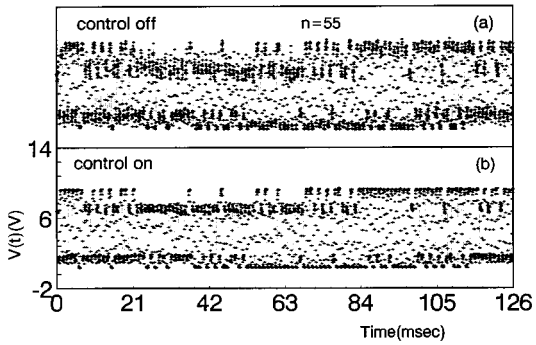

FIG. 8. Another example of experimental results of dynamic memory with the output feedback control of $F(t)=X[-V(t)]$ in the inverse bifurcation region of $m^*=2^*$. The parameters used are $T_r=41.80$ ms, $n=55$.

output feedback control, where both the chaotic and the steady oscillation wave forms are shown for comparison. It is clear to see that these experimental results agree with theoretical simulations. Up to 55 harmonic modes ($n=55$, $m^*=2^*$) have been demonstrated in our system as shown in Fig. 8, but it is difficult for the system to operate in even higher harmonic mode because of the instability limitation from the laser source and the amplifiers used.

In conclusion, we have stabilized the chaotic code oscillation to a desired stable code oscillation successfully by the two methods proposed, delayed feedback control and output feedback control, and up to 55 harmonic modes have been reached.

ACKNOWLEDGMENT

This work was supported by a ''Nonlinear Science'' project.

[1] K. Ikeda and K. Kondo, Phys. Rev. Lett. **49**, 1467 (1982).
[2] J. Y. Gao, L. M. Narducci, L. S. Schulman, M. Squicciarini, and J. M. Yuan, Phys. Rev. A **28**, 2910 (1983).
[3] K. Ikeda and K. Matsumoto, Physica D **29**, 223 (1987).
[4] P. Davis and K. Ikeda (unpublished).
[5] P. Davis, Jpn. J. Appl. Phys., Part 2 **29**, L1238 (1990).
[6] K. Ikeda, Yukawa Institute Kyoto Report No. YITP/K-981, 1992 (unpublished).
[7] T. Aida and P. Davis, Electron. Lett. **27**, 1544 (1991).
[8] T. Aida and P. Davis, IEEE J. Quantum Electron. **28**, 686 (1992).
[9] T. Aida and P. Davis, IEEE J. Quantum Electron. **30**, 2986 (1994).
[10] J. Y. Gao, J. H. Huang, Z. R. Zheng, Y. Jiang, Y. Zhang, and G. X. Jin, Opt. Eng. (Bellingham) **34**, 790 (1995).
[11] K. Pyragas, Phys. Lett. A **170**, 421 (1992).
[12] K. Pyragas and A. Tamasevicius, Phys. Lett. A **180**, 99 (1993).